



Eximia Journal
(ISSN 2784-0735)

Vol. 13

2024

Exploration of Structural and Physical Characteristics of a Ceramic-Based System via Flame Thermal Spraying

Farah S. Khasrw¹, Aya N. Abdullah², Salih Y. Darweesh³

¹Ministry of Education, Rusafa Second Directorate, Al- Takhi Secondary School for Girls, Baghdad, Iraq, ²Physics Department, College of Education For Pure Science, Kirkuk University, Kirkuk, Iraq, ³Physics Department, College of Science, Tikrit University, Tikrit, Iraq

Farah.Sadek1204a@ihcoedu.uobaghdad.edu.iq , ayanabel@uokirkuk.edu.iq,
salih.younis@tu.edu.iq

Abstract. Flame thermal spraying is an important technique in surface treatment of many materials exposed to external corrosion, including turbine blades in power plants, bridges, and oil pipelines. Therefore, a ceramic material represented by aluminum oxide Al_2O_3 was used as a base material and copper metal Cu was added at different reinforcement ratios of 5%, 10%, 15%, 20%, 25%Wt. To form a cermet alloy. The two powders were mixed after taking into account the copper concentrations, and the mixture was placed in the flame thermal spraying device crucible. The acetylene gas ratio was fixed at 0.7 bar and oxygen at 4 bar as the best mixing ratios obtained. The coating process was carried out on out-of-service turbine blade bases with dimensions of 20mm×5mm in a circular shape. After completing the coating process, the samples were sintered in a thermal oven at 1100°C for only one and a half hours. The scanning electron microscope (SEM) of the samples was examined and it was found that by adding copper we get a regular and homogeneous structure, and it was found that the best reinforcement with metal is 25% Wt. After sintering, it was also found that the average grain size is approximately 109nm. An EDX spectroscopy was also conducted to show the materials that were mixed for both alumina and copper. Some mechanical properties were also examined which showed that the best mixing ratio is (75%Wt. Al_2O_3 -25%Wt.Cu) after sintering, at which the micro-Vickers hardness was found to be (605 kg/mm²), and the wear rate was calculated which gave the lowest value (1.84×10⁻⁶g/cm). While the adhesive strength was calculated for a coated and uncoated sample to find that the best mechanical adhesive strength is (53 MPa). The true porosity and water absorption were calculated to give the lowest values at the lowest reinforcement ratio which is 25% Wt.

Keywords. Adhesion, Cermet, Porosity, SEM

1.Introduction:

Flame thermal spraying technology has a scientific history that began in the late nineteenth century and extends to the present time, where the beginnings were on metal bases for the process to develop into treating metal and steel surfaces[1]. Cermet materials, which consist of ceramic and metal in a mixture, were also used to be coated on surfaces suffering from cracks and pores, thus improving the mechanical properties as well as withstanding harsh

conditions of temperature, pressure and corrosion[2,3]. Ceramic materials require high temperatures, unlike metals, and thus the mixing process between the two materials works to combine the physical and mechanical properties, thus producing materials with high durability and giving properties that can be applied in materials exposed to high temperatures such as aviation and space and in turbine blades that are exposed to high temperatures in power plants and in many different industries[4,5].

Thermal spraying techniques vary to include plasma thermal spraying, high-speed oxygen fuel spraying, electric arc spraying, blast spraying, and flame thermal spraying[6]. Each technique has advantages and disadvantages, and the best of these techniques is plasma thermal spraying because it gives very low porosity, high velocity of molten particles, and high adhesion strength compared to other techniques, but the financial cost of the device is high, so we resort to techniques that are relatively low in cost with acceptable results within the scientific path[7,8]. Also, the transportation process and ease of working with these techniques differ according to the industrial requirement, for example, the plasma thermal spraying device needs a whole room to contain the device, and the coating process is somewhat complicated as there is difficulty in controlling the high energy needed by the plasma, and difficulty in controlling temperatures, in addition to the need for training and experience [9].

Flame spraying technology was a simple technology in terms of size, control, and cost [10]. This technology consists of two oxygen and acetylene cylinders with a thermal spray gun containing an upper crucible for the purpose of carrying the powders to be coated [11]. This technology provides many properties, including surface resistance to corrosion, improved heat resistance, improved properties of the coated surface, increased life of the coating on the surface, and reduced economic costs [12]. Flame spraying technology can coat many powders that may be metallic, ceramic, or a mixture of ceramic and metal, which is cermet [13]. Aluminum oxide is one of the ceramic materials that provides high resistance, scratch resistance, and tolerance to high temperatures with flame spraying technology, especially if mixed with another metal [14]. Many other ceramic materials can also be used, such as zirconia ZrO_2 , silicon carbide SiC , tungsten carbide WC , silicon nitride Si_3N_4 , and other different materials [15]. Therefore, the compatibility of the materials used physically and mechanically, as well as the required application, must be taken into consideration in the flame thermal spraying technique.

2. Aim of the Study:

The aim of the study is to improve the surface properties in terms of structural composition by studying the results of scanning electron microscopy (SEM) and X-ray diffraction spectroscopy (EDX) and knowing the consistency of the coated particles and their interaction with each other. Also, determining the quality of the hardness of the resulting coating and its resistance to scratching and knowing the rate of frictional wear, in addition to evaluating the mechanical adhesion strength and determining the porosity ratio and the amount of water absorption of the surface resulting from the coating.

3. Raw Materials:

The primer coating material was made of equal proportions of Al-Ni powders produced by Amdry, USA, with a purity of 99.8% and a particle size of $53\mu m$. The matrix coating material was alumina Al_2O_3 produced by (Rio Tinto Alcan), Canada, with a purity of 99.9% and a particle size of $75\mu m$, while the reinforcement material was copper powder produced by Metal

Powder Industries Federation (MPIF), USA, with a purity of 99.9% and a particle size of 100 μ m.

4. The Practical Side of the Study:

The coating process for the prepared samples was carried out by the flame thermal spraying method using a device of type (GH- 4/h) of Chinese origin. The coating parameters were determined to be shown in table (1). The metal ratios of copper were determined as 5%, 10%, 15%, 20%, 25%Wt. with the matrix material of alumina at ratios of 95%, 90%, 85%, 80%, 75%Wt. The mixing process was carried out for both the base material and the reinforcement by a locally made mixer. After that, the coating bases were prepared, which were from a turbine blade out of service from the power stations and were cut into dimensions of 20mm \times 5mm in a circular shape. The bases were roughened to ensure the adhesion of the molten powder drops to the base. Initially, the base is heated for a short time to avoid sudden expansion and contraction, i.e. to get rid of any possible thermal stress. Then, the primary bonding material of (Al-Ni) powders is coated in equal proportions, in order to benefit this coating in improving both cohesion Adhesion, where aluminum contributes to increasing cohesion while nickel contributes to increasing the adhesive strength. After completing the coating of the bonding material with a thickness of approximately 100 μ m, the two powders of Al₂O₃-Cu are coated, which are approximately 500 μ m thick. The resulting coating has a somewhat weak crystalline structure, and therefore heat treatment must be carried out using an oven containing a reducing gas such as argon to eliminate any possible oxidation processes during thermal sintering. The thermal sintering process was carried out at 1100 $^{\circ}$ C for an hour and half. The samples are left in the oven and extracted the next morning. The resulting samples need mechanical processing to be prepared for various structural and physical examinations.

Table (1) Parameters of Thermal Spraying.

| | | |
|----------------------------|---|---------------------|
| oxygen gas | 4 bar | |
| acetylene gas | 0.7 bar | |
| thickness of bonding layer | | \cong 600 μ m |
| spray angle | 90 $^{\circ}$ | |
| spray distance | 15cm | |
| The best coating | 75% Al ₂ O ₃ -25%Cu | |

5. Tests Used in the Study:

5.1. Scanning Electron Microscope (SEM) and EDX

Scanning electron microscope examination gives an idea about the surface structure of the coating material, the external appearance of the surface, and the properties of the reactants. The coating samples are cleaned, prepared, and dried in a suitable manner for the examination device. In the present study, the examination was carried out by a (MIRA3 TESCAN) scanning microscope manufactured by (TESCAN Company) of Gecko origin. The device features a wide range of lenses, a high magnification capacity of up to 1 million times, a beam voltage of up to 30Kv, analysis by X-ray spectroscopy (EDX), and the ability to analyze in three dimensions.

5.2. Vickers Hardness Test:

The Vickers hardness tester was used to calculate the hardness values of the coated samples. It is a French device that is characterized by high accuracy in finding the hardness. The samples were cleaned well and suitable for examination. The applied load was 100g, and the angle of the insertion was 136° . When the insertion is directed to the surface of the sample, it will leave a mark. By measuring the depth of the resulting mark and using the following mathematical equation [16], the hardness values for a specific place can be known through the display screen in the device. By repeating the process for different areas, the microhardness rate of the samples can be known. The process is repeated for the samples before and after thermal sintering.

$$H_V = \frac{\sin\left(\frac{136}{2}\right) \cdot 2F}{d^2} (1)$$

Where: H_V : is the Vickers hardness(kg/mm^2), F : is the effective force (load) kg, d : is the average diameter of the mark (mm^2).

5.3. Wear Rat Test:

Wear rate is used to determine the ability of materials to withstand harsh conditions of pressure, friction and corrosion under a certain load and for a certain time. One of the common methods for calculating the friction wear rate is to weigh the sample before work m_1 and after work m_2 , taking into account the weight or load as well as the number of cycles of the device and the time taken. The device used to find wear rate values is the (Pin-on-Disk Wear Tester) of Swedish origin, which contains a lower disc that rotates at a specific speed and an upper disc that holds the sample and presses with a certain force on the sample and in contact with the lower disc. The mathematical equation used to calculate the wear rate is [17,18]:

$$\text{Wear Rate}(W) = \frac{m_1 - m_2}{X} (2)$$

Where: m_1 = Weight Before Work(g), m_2 = Weight After Work(g), d = Distance Traveled by the Disk(cm).

$$X = 2\pi rn (3)$$

Where: r = The radius of the Coating Samples, n = The Number of Turns.

5.4. Adhesion Force Test:

The adhesive strength test of coated samples by flame thermal spraying is one of the common methods to determine the adhesion strength of the coating to the substrate surface. The method is performed using a substrate coated with $\text{Al}_2\text{O}_3\text{-Cu}$ and another uncoated substrate, and an epoxy adhesive is applied and left for 24 hours, after which the uncoated substrate is pulled in the opposite direction. When the two samples are pulled apart, the device records the highest adhesion strength in MPa. The device used is the (Pull-Off Adhesion Tester) from the American, company Instron. The mathematical relationship used to calculate the mechanical adhesion strength is [19]:

$$\text{Adhesion Force} = \frac{F}{A} (4)$$

Where: F = Compressive Strength(N), A = Surface area of the Coated Samples(mm^2).

5.5. Porosity Real and Water Absorption Test:

Archimedes' method is one of the most important techniques through which some physical properties can be found, including true porosity and water absorbency, which are considered an important physical property to know the percentage of pores on the surface of the

paint sample as well as the extent of the paint's absorption of water. The method consists of weighing the resulting paint while it is dry to represent the first weight m_1 , after which the sample is immersed in distilled water for 24 hours and the sample is extracted and weighted to represent the second weight m_2 , while the third weight m_3 is by weighing the sample while it is suspended in distilled water and is usually called the suspended weight. From the relationships below, both true porosity and water absorbency can be calculated[20]:

$$\text{Porosity Real\%} = \left(\frac{m_2 - m_1}{m_2 - m_3} \right) \times 100\% \quad (5)$$

Where: m_1 = Dry Weight, m_2 = Saturated Weight, m_3 = Hanging Weight.

$$\text{Water Absorption\%} = \frac{m_2 - m_1}{m_1} * 100\% \quad (6)$$

Where: w_1 = Dry Weight, w_2 = Saturated Weight.

6. Results and Discussions:

6.1. Scanning Electron Microscope SEM and X-ray Spectroscopy EDX Results

The topography of the coated surface was studied by the flame thermal spray method and for samples reinforced with different proportions of copper metal Cu on a base of alumina Al_2O_3 . The test was conducted for the samples after the thermal sintering process at 1100°C for an hour and a half. Figure (1) shows images of the scanning electron microscope and X-ray energy analysis after thermal sintering and at a resolution of 500nm and a magnification of 50KX. The figure shows the five concentrations of copper on an alumina substrate and shows that increasing the proportions of the reinforcement material contributes effectively to improving the surface topography. At low proportions, we notice the presence of some pores as in figure (1-a) which gradually disappear with increasing proportions as in figure (1-e), where we notice an improvement in the cohesion and surface adhesion because copper acts as a suitable bonding material during coating [21], especially since the temperature of the spray gun reaches approximately 3000°C , which is a temperature sufficient to melt the copper granules that merge with the alumina, thus forming a cohesive cermet surface [22]. Copper also increases flexibility, which contributes to improving the mechanical and thermal properties of the coating, which contributes to reducing cracks in the surface layer [23]. Copper can also contribute to increasing thermal distribution, as copper is a good conductor of heat, and thus we obtain a regular, consistent, less wrinkled and more aesthetic surface [24]. As shown, we find that the best mixing ratio is 25% Wt. At this point, a surface with high mechanical and physical interlocking is obtained. The proportions of the materials entering the reaction can also be known through the energy X-ray diffraction analysis test (EDX) corresponding to Figure (1-e), where copper and alumina appear clearly without any noticeable impurities.

Figure (2) shows SEM images for the same added copper concentrations. The images show the sizes of the particles participating in the reaction at nanoscale, and the nanoscale particle size can be calculated for each added ratio. Thus, when extracting the average nanoscale particle size, it was found to be approximately 109nm. The reason for the transformation of the particles into nanoscale can be attributed to several reasons, including the chemical and physical reactions occurring between copper and alumina during the melting of the particles. The effect of sudden cooling also has an effect on the transformation of the particles into nanoscale due to the complete melting of the powders, as well as the effect of high pressure and temperature, which has a significant effect on the structure and composition of the materials involved in the reaction[25].

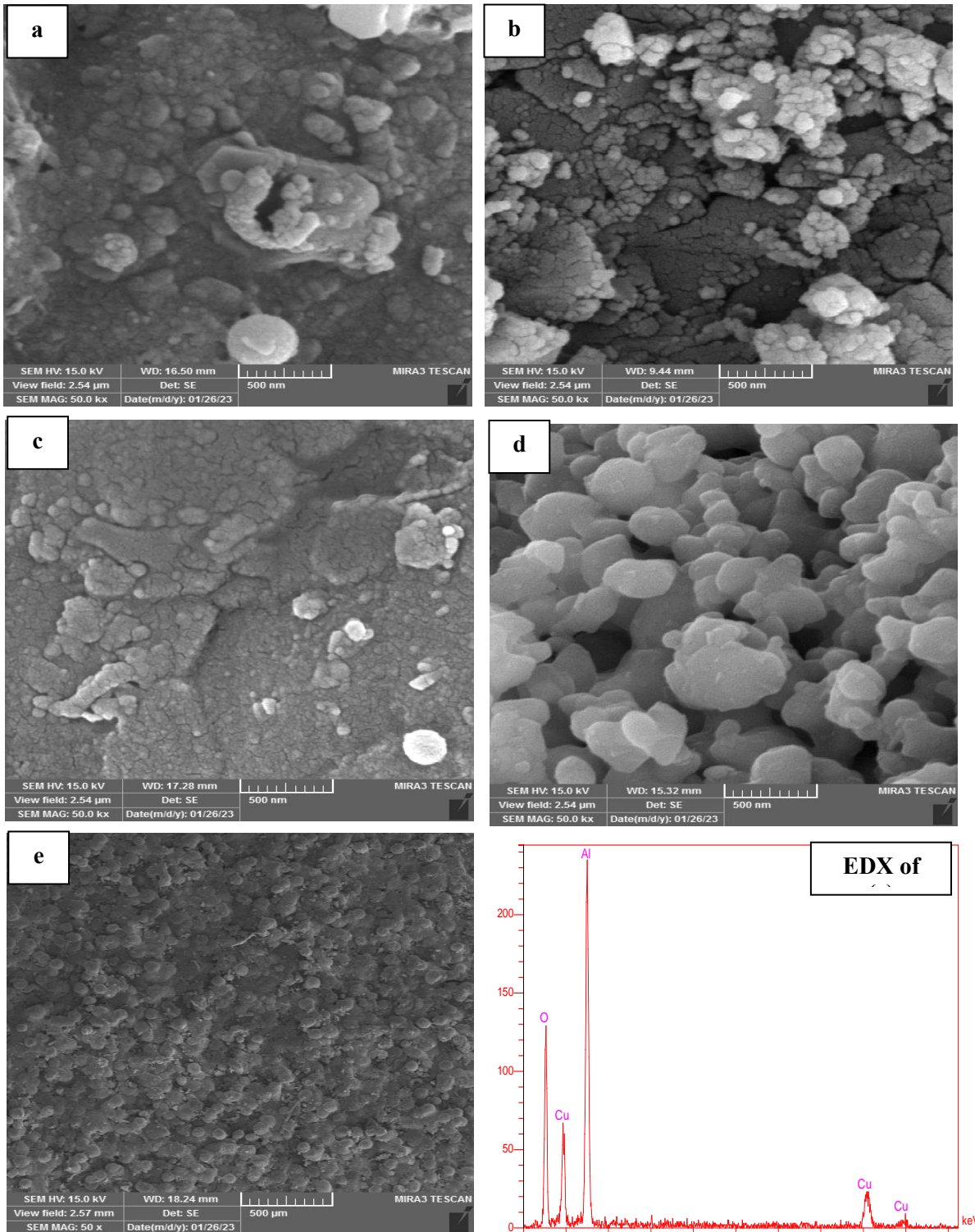


Figure (1) Scanning electron microscope (SEM) images and energy-dispersive X-ray (EDX) analysis of alumina base and copper metal reinforcement at ratios of (a-5%, b-10%, c-15%, d-20%, e-25% Wt.) after thermal sintering.

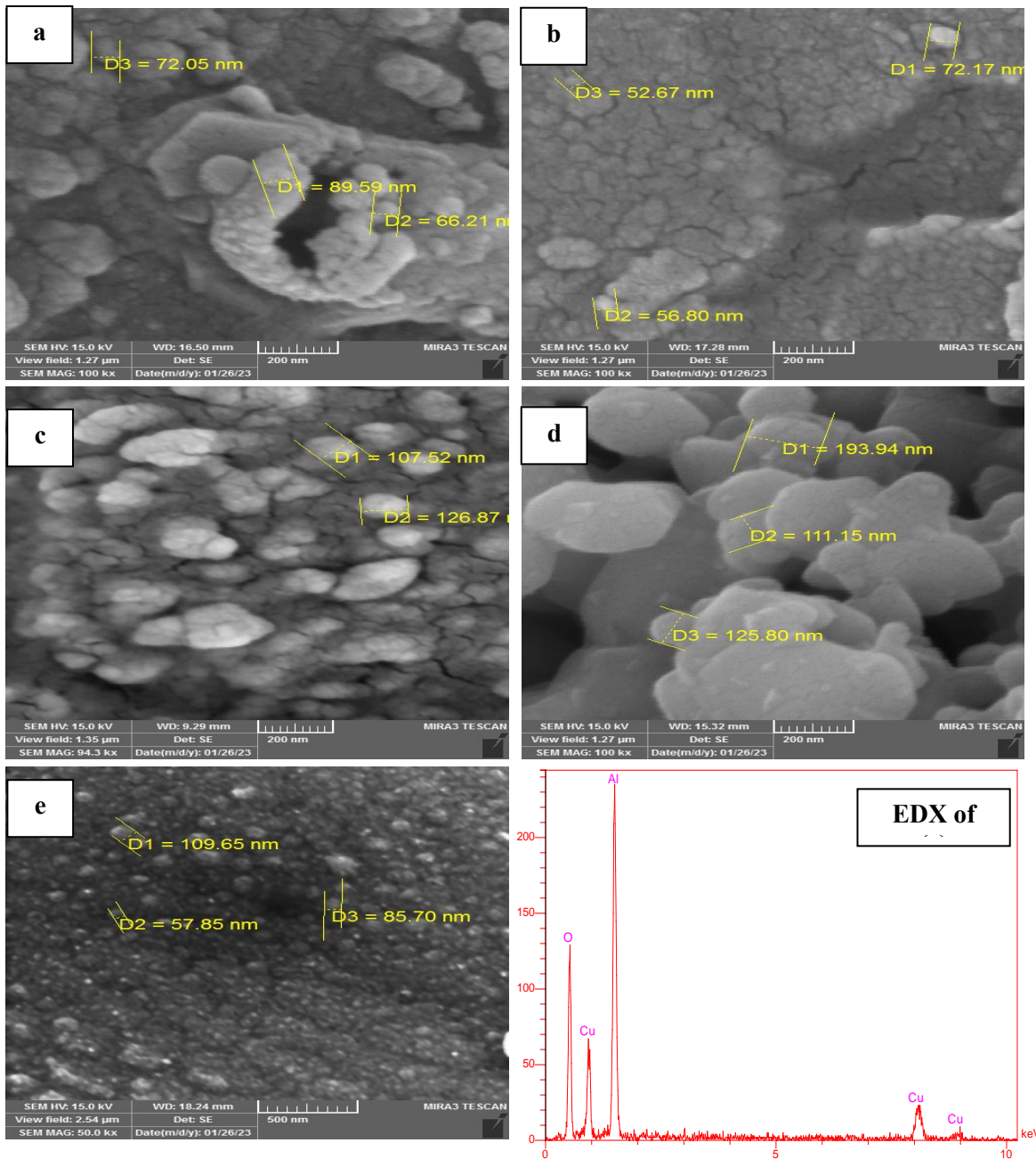


Figure (2) Scanning electron microscope (SEM) images and energy-efficient X-ray (EDX) analysis to calculate the grain size of an alumina base and copper metal reinforcement at ratios of (a-5%, b-10%, c-15%, d-20%, e-25% Wt.) after thermal sintering.

6.2. Vickers Hardness Results:

Figure (3) shows the relationship between Vickers hardness and the different addition ratios of copper metal before and after thermal sintering, as we find that the best mixing ratio of the metal reinforcement material is 25% Wt. Before and after sintering. The hardness value before sintering was 468 kg/mm², while the hardness after sintering was 605 kg/mm². This increase in the micro hardness values, which is directly proportional to the added copper ratios, is attributed to the spread and distribution of copper metal on the alumina floor, thus forming a mixed composition of copper and alumina with a high hardness that exceeds the hardness of pure alumina. The high density of copper also contributes to increasing the hardness in terms

of the size distribution of particles and high density [26]. As for thermal sintering, we notice an improvement in the hardness, which is due to the importance of sintering in smoothing the outer surface and merging and reducing pores, in addition to getting rid of cracks that occur during coating [27]. In general, we find that the effect of copper is clear through its work as a binding material that helps in the cohesion between the particles, and it also led to improving the mechanical properties of the cermet coating while improving the crystalline structure of the system as a whole[28].

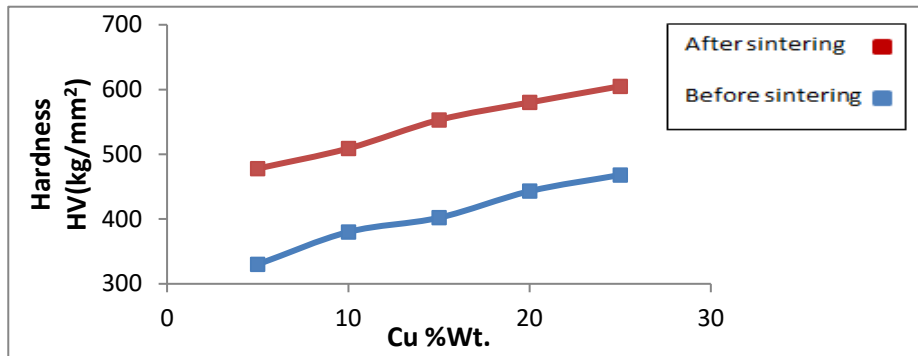


Figure (3) The relationship between Vickers hardness and different copper addition ratios before and after thermal sintering.

6.3. Wear Rate Results:

Figure (4) shows the relationship between the wear rate and the percentages of copper addition before thermal sintering, as it shows that the value of the wear rate decreased with copper additions to be at the best result at a percentage of 25% Wt., as it reached $(1.74 \times 10^{-4} \text{ g/cm})$. As for figure (5), it shows the relationship between the wear rate and the percentages of copper addition after thermal sintering, as the best copper mixing ratio was obtained at 25% Wt., which gives the lowest wear rate, which is $(1.84 \times 10^{-6} \text{ g/cm})$. Thus, we conclude that the repeated addition of copper contributed to reducing the wear rate, especially after thermal sintering. This behavior can be interpreted as an improvement in the crystalline structure as well as an improvement in the surface hardness of the coating, which in turn led to a reduction in the wear rate, which shows the possibility of using this coating in industries that are exposed to pressure and load force with the presence of heat, such as turbine blades [29]. The addition of copper also helped to form compounds with strength and hardness with resistance to corrosion during operation in terms of increasing mechanical properties [30]. The effect of thermal sintering is clear on the paint samples, which in turn helped reduce surface defects and increase the density of the material, thus leading to increased hardness, as sintering also contributes to making the material withstand mechanical pressures and friction[31].

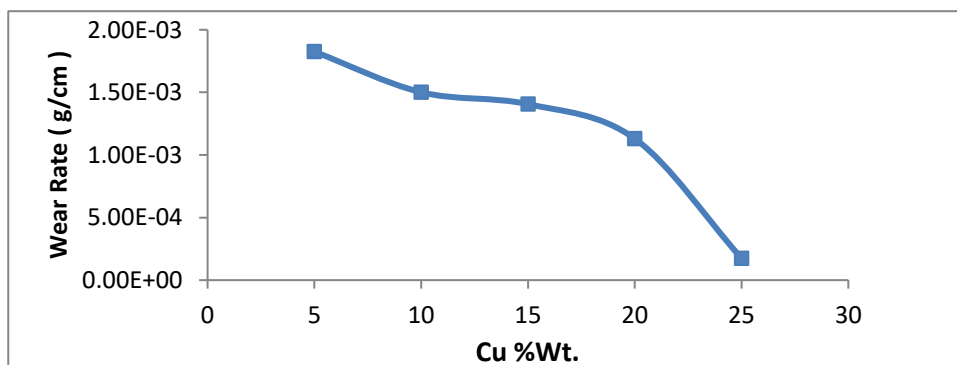


Figure (4) The relationship between the friction wear rate and the different copper addition ratios before thermal sintering.

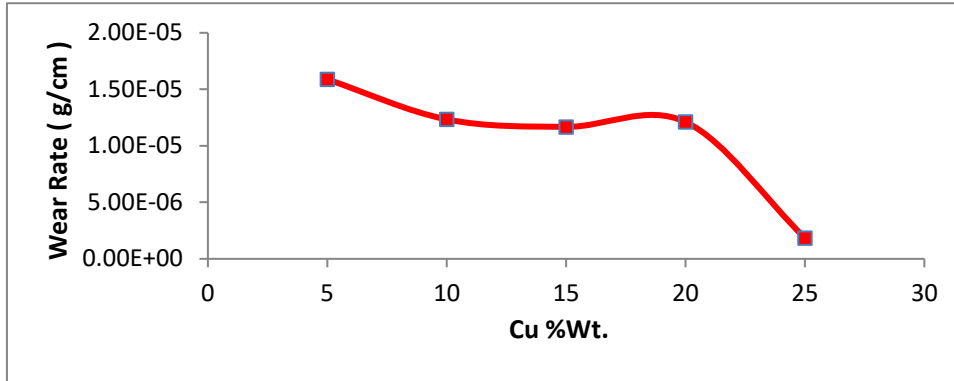


Figure (5) The relationship between the friction wear rate and the different copper addition ratios after thermal sintering.

6.4. Adhesion Force Results:

Figure (6) shows the relationship between the mechanical adhesion strength with the repeated copper addition ratios before and after sintering. It is clear that the best mixing ratio obtained for copper is 25% Wt. This is the best mixing ratio obtained from the above results, if it is found that the value of the adhesion strength before sintering at the above ratio is 33MPa, while this ratio increased to be 53MPa after thermal sintering. The reasons for the increase in the adhesion strength are attributed to the improvement of the physical and chemical properties as a result of the increased interaction and convergence between the particles during the recrystallization process[32]. Also, the coating distance between the coating gun and the steel base is suitable for the molten droplets to reach the base while they are hot, which gives them enough time to merge and interact with the rest of the previous droplets, as well as the roughening method of the base, which contributed to the good cohesion between the droplets and the base[33]. The sizing and increasing the interaction between hot droplets is very important than if the droplets are cold, because the flattening and merging process will be small if the coating distance is large. Also, thermal sintering has a great effect on recrystallizing the surface grains and improving the roughness of the outer surface, as the smoother the surface, the higher the adhesion strength [34]. Also, the angle of the coating with the paint gun has a great effect, as the vertical angle of 90° gives a coating with an almost even surface, unlike the oblique angles that give coatings with varying thicknesses. Thus, when the coating was carried out at a vertical angle, it gave high hardness and adhesion strength [35].

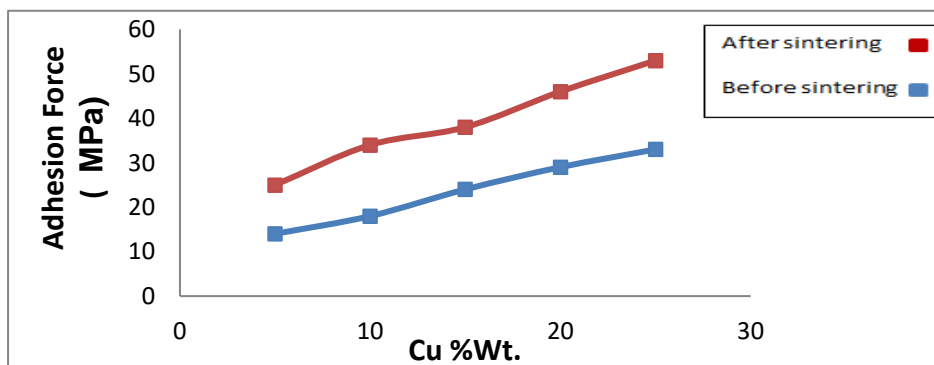


Figure (6) The relationship between the adhesion strength and the different copper addition ratios before and after thermal sintering.

6.5. Porosity Real and Water Absorption Results:

Figure (7) shows the relationship between the actual porosity and the addition ratios of copper metal before and after thermal sintering. We find that the best ideal mixing ratio is 25% Wt. of copper, which is what was obtained by all the mechanical tests above. The porosity value before thermal sintering was found to be 11%, while after thermal sintering it was 5.5% at the same ideal added copper ratio. Therefore, the decrease in porosity with the continued addition of copper is due to the behavior of copper metal in terms of high density and filling the open pores during the coating process, as copper granules work to bind the interacting components with each other and block the generated bubbles[36]. The heat treatment process also affected the treatment of some of the air gaps formed during coating and thus reduced the percentage of pores. Also, high temperatures work to recrystallize and rearrange the particles between copper and alumina[37]. It is also possible to form a liquid of copper metal that can extend between the pores, fill them, reduce their number, and remove the formed crystalline defects [38].

Figure (8) shows the relationship between the water absorption ratio with different copper additives before and after thermal sintering. As is known in the current study, the best copper mixing ratio is 25% Wt., at which it was found that the water absorption before sintering is 1.25%, which decreased after thermal sintering to 0.81%. This behavior in the decrease in water absorption values is attributed to several reasons, the most important of which is the decrease in pores that may contain water and increase water absorption, as well as the presence of copper, which is considered a filling and binding factor that contributes to reducing absorption values, and also heat treatment, which contributed to reducing pores and thus reducing water absorption [39]. Also, the coating that contains a water absorption ratio higher than 1% is considered a porous coating, while the coating that contains a water absorption ratio of less than 1% is considered a glazed coating, and here after thermal sintering, a glazed coating was obtained [40].

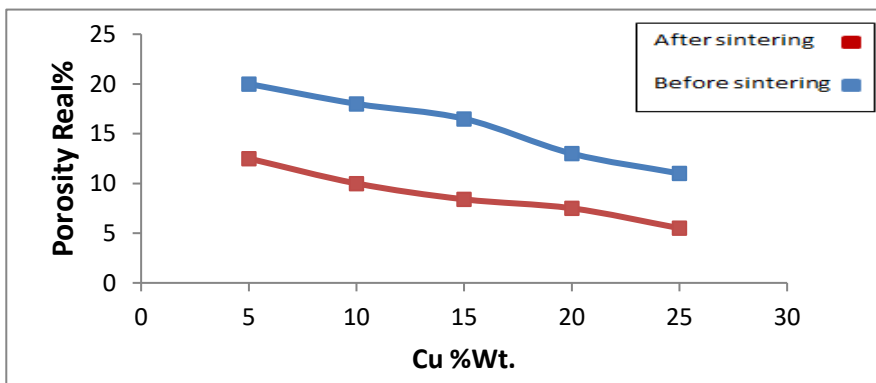


Figure (7) The relationship between the true porosity and the different copper addition ratios before and after thermal sintering.

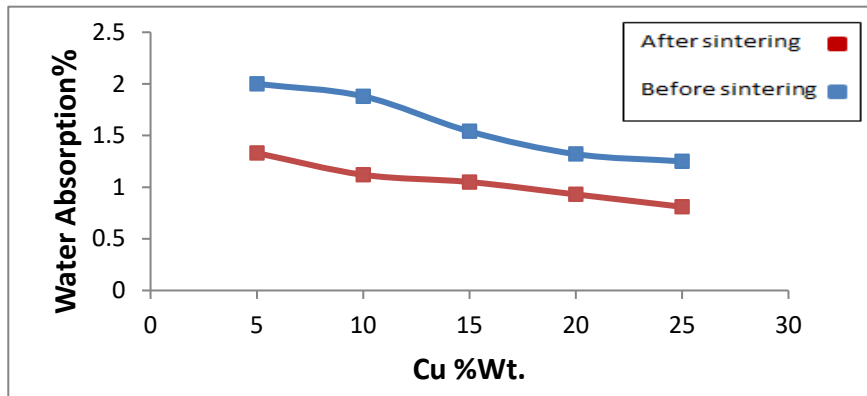


Figure (8) The relationship between water absorption and different copper addition ratios before and after thermal sintering.

7. Conclusions:

The present study shows the possibility of cermet coating from the ($\text{Al}_2\text{O}_3\text{-Cu}$) system, with a clear improvement in the structural, mechanical and physical properties of the system, if the best ideal mixing ratio is obtained, which is (75% Wt. $\text{Al}_2\text{O}_3\text{-25% Wt. Cu}$). The scanning electron microscope results showed a clear regularity on the coating surface with mechanical and interlocking interference between the coated components. The mechanical results gave the highest hardness and the highest mechanical adhesion strength with the lowest possible wear rate at the same ideal mixing ratio, while the physical results showed a decrease in the values of true porosity and water absorption in inverse proportion to the copper addition ratios. In general, we conclude that the resulting coating layer can be used to treat equipment exposed to harsh conditions of corrosion, high pressure and temperature, such as turbine blades, missile bases and space applications.

References:

- [1] Pawlowski, L. (2008). The science and engineering of thermal spray coatings. John Wiley & Sons.
- [2] El Rayes, M. M., Abdo, H. S., & Khalil, K. A. (2013). Erosion-corrosion of cermet coating. *International journal of electrochemical science*, 8(1), 1117-1137.
- [3] Tiwari, A., Seman, S., Singh, G., & Jayaganthan, R. (2019). Nanocrystalline cermet coatings for erosion–corrosion protection. *Coatings*, 9(6), 400.
- [4] Abdullah, M. A., Hadi, R. Z., & Darweesh, S. Y. (2024). Protection of turbine blades by adding metals to ceramic materials using flame coating method. *Journal of King Saud University-Engineering Sciences*.
- [5] Darweesh, S. Y., Rasheed, R. A., & Abdullah, M. A. (2023). Treatment of Failures in Turbine Blades by Cermet Coatings. *Journal of Failure Analysis and Prevention*, 23(6), 2461-2470.
- [6] Fauchais, P. L., Heberlein, J. V., Boulos, M. I., Fauchais, P. L., Heberlein, J. V., & Boulos, M. I. (2014). Industrial applications of thermal spraying technology. *Thermal Spray Fundamentals: From Powder to Part*, 1401-1566.
- [7] Darweesh, S. Y., Jassim, A. H., & Taha, A. O. (2023, December). Enhancement some physical properties of metal-based composites reinforced with carbide materials by

- thermal spray method. In AIP Conference Proceedings (Vol. 2977, No. 1). AIP Publishing.
- [8] Ahmed, M. N., Daham, N. A., & Darweesh, S. Y. (2024, March). Structural and mechanical properties for (Ni-WC) system by using thermal spray. In AIP Conference Proceedings (Vol. 2885, No. 1). AIP Publishing.
- [9] Vardelle, A., Moreau, C., Themelis, N. J., & Chazelas, C. (2015). A perspective on plasma spray technology. *Plasma Chemistry and Plasma Processing*, 35, 491-509.
- [10] Trommer, R. M., & Bergmann, C. P. (2015). *Flame Spray Technology: Method for Production of Nanopowders*. Springer.
- [11] Henao, J., Poblano-Salas, C. A., Vargas, F., Giraldo-Betancur, A. L., Corona-Castuera, J., & Sotelo-Mazón, O. (2021). Principles and applications of thermal spray coatings. In *Advanced Surface Coating Techniques for Modern Industrial Applications* (pp. 31-70). IGI Global.
- [12] Lakkannavar, V., Yogesha, K. B., Prasad, C. D., Mruthunjaya, M., & Suresh, R. (2024). A review on tribological and corrosion behaviour of thermal spray coatings. *Journal of The Institution of Engineers (India): Series D*, 1-17.
- [13] Antar, R. S., Darweesh, S. Y., & Ridha, F. W. (2024). Production of a double cermet coating to treatment of the turbine blades. *Engineering Research Express*, 6(1), 015407.
- [14] Roshan, R., Patel, S. K., & Behera, A. (2024). Future perspective of ceramic coating. In *Advanced Ceramic Coatings for Energy Applications* (pp. 325-341). Elsevier.
- [15] Treccani, L. (2023). *Introduction to Ceramic Materials. Surface-Functionalized Ceramics: For Biotechnological and Environmental Applications*, 1-46.
- [16] Alemzadeh, J. (2024). *Exploiting the properties of graphene to improve the mechanical and functional properties of ceramic-based materials* (Doctoral dissertation, Cardiff University).
- [17] Kurtz, S. M., Holyoak, D. T., Trebše, R., Randau, T. M., Porporati, A. A., & Siskey, R. L. (2023). Ceramic Wear Particles: Can They Be Retrieved In Vivo and Duplicated In Vitro?. *The Journal of arthroplasty*, 38(9), 1869-1876.
- [18] Hamoudi, M. S., Mahmoud, A. S., & Darweesh, S. Y. (2024, March). Study of the effect of grinding time for a compound (Al-Ni-Mgo) on the values of hardness, compressive strength and wear rate using powder technology. In AIP Conference Proceedings (Vol. 2885, No. 1). AIP Publishing.
- [19] Mushtaq, M., Adusumalli, R. B., Suresh, K., & Anna Abraham, A. (2023). Adhesion and tribological characteristics of modified polyurethane coating on composite substrate. *Surface Engineering*, 39(7-12), 836-851.
- [20] Monticeli, F., Voorwald, H., & Cioffi, M. O. (2021, October). Porosity Measurement in Carbon-Fiber-Reinforced Polymer Composite Through Optical Microscopy Using ImageJ Software. In *International Conference on Advanced Mechanical and Power Engineering* (pp. 265-273). Cham: Springer International Publishing.
- [21] Wei, H., Xia, J., Zhou, W., Zhou, L., Hussain, G., Li, Q., & Ostrikov, K. K. (2020). Adhesion and cohesion of epoxy-based industrial composite coatings. *Composites Part B: Engineering*, 193, 108035.
- [22] Boulos, M. I., Fauchais, P. L., Heberlein, J. V., Boulos, M. I., Fauchais, P. L., & Heberlein, J. V. (2021). Industrial applications of thermal spray technology. *Thermal Spray Fundamentals: From Powder to Part*, 997-1096.

- [23] Jia, Y., Zhou, K., Sun, W., Ding, M., Wang, Y., Kong, X., ... & Fu, Y. (2024). Enhancement mechanisms of mechanical, electrical and thermal properties of carbon nanotube-copper composites: A review. *Journal of Materials Research and Technology*.
- [24] Barani, Z., Mohammadzadeh, A., Geremew, A., Huang, C. Y., Coleman, D., Mangolini, L., ... & Balandin, A. A. (2020). Thermal properties of the binary-filler hybrid composites with graphene and copper nanoparticles. *Advanced Functional Materials*, 30(8), 1904008.
- [25] Li, P., Dong, C., & Zhang, L. (2024). Mechanistic investigation of nucleation kinetics in heterogeneous ice crystallization: the role of cooling rate, surface energy, surface nanostructure, and wetting state. *International Journal of Heat and Mass Transfer*, 232, 125939.
- [26] Zhou, C., Gong, C., Wang, Z., & Tian, X. (2024). Effect of Particle Incident Angle on the Hardness and Thermal Conductivity of Cu Coating Applied to a Cr-Zr-Cu Substrate using High-Pressure Cold Spray. *Journal of Materials Engineering and Performance*, 1-12.
- [27] Qadir, D., Sharif, R., Nasir, R., Awad, A., & Mannan, H. A. (2024). A review on coatings through thermal spraying. *Chemical Papers*, 78(1), 71-91.
- [28] Mouhson, E. H., Humeedi, S. H., Darweesh, S. Y., & Ahmed, A. R. (2021). Treatment of Turbine Blades via Cr₂O₃-Ni5% Al System Using Plasma Thermal Spraying. *Journal of King Faisal University: Basic and Applied Sciences*, 22(2), 120-4.
- [29] Mourad, A. H. I., Almomani, A., Sheikh, I. A., & Elsheikh, A. H. (2023). Failure analysis of gas and wind turbine blades: A review. *Engineering Failure Analysis*, 146, 107107.
- [30] Veerappan, G., Ravichandran, M., Mohanavel, V., Pritima, D., & Rajesh, S. (2023). Effect of copper on mechanical properties and corrosion behavior of powder metallurgy processed Ni-Co-Cr-Fe-Mn-Cu x high entropy alloy. *Arabian Journal for Science and Engineering*, 48(3), 2905-2915.
- [31] Xie, S., Song, C., Yu, Z., Liu, S., Lapostolle, F., Klein, D., ... & Liao, H. (2021). Effect of environmental pressure on the microstructure of YSZ thermal barrier coating via suspension plasma spraying. *Journal of the European Ceramic Society*, 41(1), 535-543.
- [32] Imbriglio, S. I., & Chromik, R. R. (2021). Factors affecting adhesion in metal/ceramic interfaces created by cold spray. *Journal of Thermal Spray Technology*, 1-21.
- [33] Govande, A. R., Chandak, A., Sunil, B. R., & Dumpala, R. (2022). Carbide-based thermal spray coatings: A review on performance characteristics and post-treatment. *International Journal of Refractory Metals and Hard Materials*, 103, 105772.
- [34] Pan, C., Zhang, J., & Li, S. (2024). Review of Surface Treatment Technology for Improving Wear Resistance of Magnesium Alloys. *Recent Patents on Engineering*, 18(8), 102-122.
- [35] Heidarinejad, A., & Ashrafizadeh, F. (2024). Influence of surface texture and coating thickness on adhesion of nickel plated coatings to aluminium substrate. *Journal of Manufacturing Processes*, 120, 435-448.
- [36] Liu, P., & Chen, G. F. (2014). *Porous materials: processing and applications*. Elsevier.
- [37] Tian, B., Liu, P., Song, K., Li, Y., Liu, Y., Ren, F., & Su, J. (2006). Microstructure and properties at elevated temperature of a nano-Al₂O₃ particles dispersion-strengthened copper base composite. *Materials Science and Engineering: A*, 435, 705-710.

- [38] Hidalgo-Manrique, P., Lei, X., Xu, R., Zhou, M., Kinloch, I. A., & Young, R. J. (2019). Copper/graphene composites: a review. *Journal of materials science*, 54, 12236-12289.
- [39] Karim, A. S., Majeed, Z. N., & Darweesh, S. Y. (2021, August). The Effect of Nanostructured Zirconia Reinforcement on the Mechanical and Structural Properties of a Copper-Based System. In *Materials Science Forum* (Vol. 1039, pp. 297-306). Trans Tech Publications Ltd.
- [40] Darwish, S. Y., & Majid, Z. N. (2020). Improving the Durability of Streak and Thermal Insulation of Petroleum Pipes by Using Polymeric Based Paint System: Polymer Matrix Composites have several and wide applications. *Baghdad Science Journal*, 17(3), 0826-0826.